11th World Congress on Computational Mechanics (WCCM XI)
5th European Conference on Computational Mechanics (ECCM V)
6th European Conference on Computational Fluid Dynamics (ECFD VI)
E. Oñate, J. Oliver and A. Huerta (Eds)

MODIFYING RESONANCE MODES OF DISSIPATIVE STRUCTURES USING MAGNITUDE AND PHASE INFORMATION

Hugo J. Peters*†, Paolo Tiso*, Johannes F.L. Goosen* and Fred van Keulen*

* Structural Optimization and Mechanics, Delft University of Technology,
Mekelweg 2, 2628 CD Delft, The Netherlands
e-mail: {h.j.peters-1, p.tiso, j.f.l.goosen, a.vankeulen }@tudelft.nl

†DevLab, Development Laboratories,
Horsten 1, MMP 0.10, 5612 AX Eindhoven, The Netherlands

Key words: Non-proportional damping, Eigensolution modification, Local structural changes, Modal modulus and argument

Abstract.

Several Flapping Wing Micro Air Vehicle (FWMAV) designs exploit structural resonance to decrease power consumption. Practical use of most resonating structures requires temporary modifications to the resonance mode (i.e., the eigensolution). This paper presents a systematic design approach to modify non-proportionally damped resonance modes in a desired way while consuming minimal control power. These modifications are induced by local structural changes. Eigensolution sensitivities in the modal basis are used to linearly approximate the effect of these changes on the resonance mode. Results show that the interpretation of resonance mode changes is highly clarified by introducing the modulus (magnitude) and argument (phase) information of the resonance mode. The proposed projection allows the determination of the locations at which a specific structural change scores maximum effect in terms of relative magnitude and/or phase modifications. The applied modal approach reduces the size of the problem, which is advantageous during analysis. This work shows resonance mode modifications of non-proportionally damped systems due to local structural changes in a intuitive manner.

1 INTRODUCTION

Structural resonance can be exploited in mechanical applications to obtain a specific motion at relatively low actuation power [1]. At resonance there is, ideally, only energy dissipated by damping and this energy should be compensated for by the input excitation. Based on the intentional use of resonance within nature [2], several Flapping Wing Micro

Air Vehicle (FWMAV) designs mimic the resonating thorax structure of insects to increase energy efficiency [3, 4]. These designs use structural resonance properties to achieve the desired flapping motion of the wings. The damping acting on these designs is primarily caused by the aerodynamics and is therefore localized around the wings. Hence, these FWMAV designs can be seen as non-proportionally damped resonating structures.

A FWMAV design, and many other applications, require some form of control by temporary modifying the resonance mode. Resonance modes are determined by structural properties (i.e., mass, damping, stiffness and their spatial distribution) such that the resonance mode modifications can be controlled by introducing local structural property changes. These local structural changes can be induced by attaching actuators (e.g., piezoelectric patches) to the structure [5]. To modify resonance modes effectively, we search for the optimal location to induce structural changes to achieve substantial resonance mode modifications with minimal control power consumption.

Sensitivity analysis can be used to linearly approximate the change of the resonance mode (i.e., eigenvalue and eigenmode) due to local structural changes. Although the eigenvalue sensitivity is straightforward, the eigenmode sensitivity is more involved. For undamped systems, a modal method has been presented which expresses the eigenmode sensitivities as a linear combination of the eigenmodes [6] while another method requires only the eigenmode of interest [7]. These methods have been extended to allow for eigensolution sensitivities of viscously damped [8, 9, 10] and non-viscously damped systems [11, 12]. Eigensolution sensitivity analysis has been combined with optimization techniques to design undamped vibrating structures that target desired resonance modes [13, 14, 15]. Additionally, eigensolution sensitivities are employed to indicate the effect of temporary local structural modifications on resonance modes [16]. The latter uses the modal basis of the structure to increase intuitive insights.

However, studies on the (temporary) control of eigensolutions have been focusing on undamped systems. Hence, systematic ways to modify resonance modes of (non-proportionally) damped systems using local structural changes are not addressed in literature. This paper presents a systematic design approach to modify non-proportionally damped resonance modes in an insightful way using local structural changes while consuming minimal control power.

This work focuses on eigensolution (i.e., eigenvalues and eigenmodes) modifications since they mainly determine the resonance configuration. The eigenvalues are assumed to be nonzero (i.e., no rigid body modes) and distinct (i.e., no repeated eigenvalues). As a first step, the damping is assumed to be viscous. A modal basis is used as the preferred basis to provide more intuitive understanding and maximum insight.

This paper is organized as follows. Section 2 presents the systematic approach to modify eigensolutions in the desired way. The relative modulus (magnitude) and argument (phase) of the resonance modes are determined to clarify the interpretation. In Section 3 we illustrate the presented systematic approach on a simple N-dof mass-spring-damper system. Section 4 presents conclusions and suggestions for future research.

2 METHOD

This section presents an approach to describe non-proportionally damped resonance mode modifications due to local structural modifications. Firstly, we show the damped eigenproblem for free vibrations, followed by an interpretation of the eigenmodes. After that, we present eigensolution sensitivities due to structural changes and a projection method to modify eigensolutions in a systematic way.

2.1 Eigenproblem formulation

The dynamic equilibrium of a viscously damped system is governed by

$$\mathbf{M}\ddot{\mathbf{q}} + \mathbf{C}\dot{\mathbf{q}} + \mathbf{K}\mathbf{q} = \mathbf{p}\left(t\right), \tag{1}$$

where $\mathbf{M}$, $\mathbf{C}$ and $\mathbf{K} \in \mathbb{R}^{N\times N}$ are the mass, damping and stiffness matrix, respectively, $\mathbf{q} \in \mathbb{C}^N$ is the response vector and $\mathbf{p} \in \mathbb{R}^N$ is the excitation vector. $\mathbf{M}$ and $\mathbf{K}$ are symmetric and positive definite to exclude the presence of rigid body modes whereas $\mathbf{C}$ is symmetric and non-negative. If we assume a free vibration (i.e., when no external load $\mathbf{p}\left(t\right)$ is applied) in the form of $\mathbf{q}\left(t\right) = \mathbf{x}e^{\lambda t}$, the damped eigensolutions are defined as the solution of the damped eigenvalue problem:

$$\left(\lambda_k^2\mathbf{M} + \lambda_k\mathbf{C} + \mathbf{K}\right)\mathbf{x}_k = \mathbf{0}, \qquad \forall k = 1, \ldots, N. \tag{2}$$

In Eq. (2), $\lambda_k \in \mathbb{C}$ is the k^{th} eigenvalue and $\mathbf{x}_k \in \mathbb{C}^N$ is the corresponding eigenmode. We can put Eq. (2) into a standard first-order eigenvalue problem by casting it into the state-space form. That is,

$$\left(\lambda_k\mathbf{A} + \mathbf{B}\right)\begin{bmatrix}\lambda_k\mathbf{x}_k \\ \mathbf{x}_k\end{bmatrix} = \left(\lambda_k\mathbf{A} + \mathbf{B}\right)\mathbf{z}_k = \mathbf{0} \qquad \forall k = 1, \ldots, 2N, \tag{3}$$

$$\text{with} \quad \mathbf{A} = \begin{bmatrix}\mathbf{0} & \mathbf{M} \\ \mathbf{M} & \mathbf{C}\end{bmatrix}, \quad \text{and} \quad \mathbf{B} = \begin{bmatrix}-\mathbf{M} & \mathbf{0} \\ \mathbf{0} & \mathbf{K}\end{bmatrix}. \tag{4}$$

In Eq. (3), the eigenvalues $\lambda_k \in \mathbb{C}$ and eigenmodes $\mathbf{z}_k \in \mathbb{C}^{2N}$ appear in complex conjugate pairs. For convenience, we arrange the eigenvalues as

$$\lambda_1, \lambda_2, \ldots, \lambda_N, \lambda_1^*, \lambda_2^*, \ldots, \lambda_N^*, \tag{5}$$

where $(\bullet)^*$ denotes the complex conjugate. Repeated eigenvalues are excluded in this analysis. Since the viscous damping is assumed to be non-proportional, the eigenvalues λ_k and eigenmodes $\mathbf{x}_k$ are always complex indicating free vibration solutions which represent non-synchronous damped oscillations. As for real modes, complex modes can be scaled arbitrarily. However, the relative importance of the real and imaginary component of the complex eigenmode is brought to evidence by specific scaling. The eigenmodes are normalized using [9]

$$\mathbf{z}_k^T\mathbf{A}\mathbf{z}_k = \mathbf{x}_k^T\left[2\lambda_k\mathbf{M} + \mathbf{C}\right]\mathbf{x}_k = \frac{1}{\gamma_k}, \tag{6}$$

where $\gamma_k \in \mathbb{C}$ represents the normalization constant and $(\bullet)^T$ denotes the vector transpose. Although there are several ways to select γ_k, we choose $\gamma_k = 1/2\lambda_k$ which is most consistent with traditional modal analysis practice. This eigenmode normalization minimizes the relative contribution of the imaginary part while maximizing the the real part. Hence, the real part contains most of the information. Since damping is non-proportional, the imaginary parts of the eigenmodes is never equal to zero.

2.2 Modulus and argument of an eigenmode

Eigenmode $\mathbf{x}_k$ has a real and an imaginary part (i.e., $\mathbf{x}_k = [\Re(\mathbf{x}_k) + i\Im(\mathbf{x}_k)]$ where $\Re$ and $\Im$ indicate the real and imaginary part, respectively). Subsequently, there are two shapes which determine the complex, non-synchronous eigenmode. For a more clear and unambiguous interpretation, the modulus (magnitude) and argument (phase) of each degree of freedom (dof) of the eigenmode are determined. The modulus determines the relative vibration amplitude of each dof with respect to the other dofs. This leads to a single, real shape (i.e., comparable to an undamped real eigenmode). The argument determines the relative phase of each dof such that the phase lag/lead of a specific dof with respect to other dofs can be determined to describe the non-synchronousness of the eigenmode. The modulus of a specific dof i of eigenmode $\mathbf{x}_k$ is given by

$$[|\mathbf{x}_k|]_i = \sqrt{\left([\Re(\mathbf{x}_k)]_i\right)^2 + \left([\Im(\mathbf{x}_k)]_i\right)^2} \qquad \forall i = 1, \ldots, N, \tag{7}$$

leading to the modulus set $|\mathbf{x}_k| \in \mathbb{R}^N$ and the corresponding argument of dof i is given by

$$[\boldsymbol{\phi}_k]_i = \arctan\left(\frac{[\Im(\mathbf{x}_k)]_i}{[\Re(\mathbf{x}_k)]_i}\right) \qquad \forall i = 1, \ldots, N, \tag{8}$$

leading to the argument set $\boldsymbol{\phi}_k \in \mathbb{R}^N$. Contrary to the argument set $\boldsymbol{\phi}_k$ of the currently investigated non-proportionally damped systems, $\boldsymbol{\phi}_k$ is *constant* (i.e., the same for all dofs) for proportionally damped systems and *zero* for undamped systems.

2.3 Eigensolution sensitivities

Structural changes, as applied by control actuators, lead to eigensolution modifications. These modifications can be approximated using first order sensitivity analysis. The structural changes of the system are described by a set of m control variables, $\mathbf{s} = \{s_1, s_2, \ldots, s_m\}^T \in \mathbb{R}^m$, so that the mass, damping and stiffness matrices become functions of $\mathbf{s}$. In this section, we consider one arbitrary element of the control vector $\mathbf{s}$, s_1. For convenience, the notation $\partial(\bullet)/\partial s_1 \equiv (\bullet)'$ is used. This section presents and interprets a summary of relevant results from the research of [9] on eigensolution sensitivities in the modal basis.

Using the normalization definition (see Eq. (6)), the sensitivity of the k^{th} eigenvalue to the control variable s_1 is determined to be

$$\lambda_k' = -\gamma_k \mathbf{x}_k^T \left[\lambda_k^2 \mathbf{M}' + \lambda_k \mathbf{C}' + \mathbf{K}'\right] \mathbf{x}_k, \tag{9}$$

which clearly shows the influence of the physical changes to the structural matrices. The real part of $\lambda'_k \in \mathbb{C}$ (i.e., $\Re(\lambda'_k)$) affects the decay rate of eigenmode k during a free vibration while the imaginary part (i.e., $\Im(\lambda'_k)$) affects the damped eigenfrequency.

For the eigenmode sensitivity, we first express the eigenmode sensitivity of the first-order system (see Eq. (3)) as a linear combination of all eigenmodes $\mathbf{z}_l$. That is,

$$\mathbf{z}'_k = \sum_{l=1}^{2N} \alpha_{kl} \mathbf{z}_l, \tag{10}$$

where $\alpha_{kl} \in \mathbb{C}$ determines the contribution of eigenmode $\mathbf{z}_l$ to the sensitivity of eigenmode $\mathbf{z}_k$. The calculated contribution coefficients, α_{kl}, are of little use since they are in terms of the first-order system. By using Eqs. (3) and (4), α_{kl} for $l = 1, \ldots, 2N$ can be expressed in terms of the eigenmodes of the second-order system. Hence, the eigenmode sensitivity of the second-order system can be expressed by

$$\mathbf{x}'_k = \sum_{l=1}^{2N} \beta_{kl} \mathbf{x}_l, \tag{11}$$

where β_{kl} is given by

$$\beta_{kl} = \begin{cases} -\gamma_l \dfrac{\mathbf{x}_l^T \left[\lambda_k^2 \mathbf{M}' + \lambda_k \mathbf{C}' + \mathbf{K}'\right] \mathbf{x}_k}{(\lambda_k - \lambda_l)}, & \forall l = 1, \ldots, 2N,\ l \neq k, k+N, \quad (12) \\ -\dfrac{\gamma_k}{2} \left(\mathbf{x}_k^T \left[2\lambda_k \mathbf{M}' + \mathbf{C}'\right] \mathbf{x}_k\right), & \text{for} \quad l = k, \quad (13) \\ \dfrac{i\gamma_k^*}{2\Im(\lambda_k)} \left(\mathbf{x}_k^* - \eta_{\mathbf{x}_k} \mathbf{x}_k\right)^T \left[\lambda_k^2 \mathbf{M}' + \lambda_k \mathbf{C}' + \mathbf{K}'\right] \mathbf{x}_k, & \text{for} \quad l = k+N, \quad (14) \end{cases}$$

with

$$\eta_{\mathbf{x}_k} = \gamma_k \left(\left(\mathbf{x}_k^*\right)^T \left[\left(\lambda_k + \lambda_k^*\right) \mathbf{M} + \mathbf{C}\right] \mathbf{x}_k \right). \tag{15}$$

A careful inspection of the expressions for coefficient β_{kl} (see Eqs. (12), (13) & (14)) shows that:

- The numerator of Eq. (12) depends on the location and dimension of the structural change. This dependency is caused by the interplay between the segments of the eigenmodes $\mathbf{x}_k$ and $\mathbf{x}_l$ and the sensitivity of the structural matrices corresponding to the locations at which the structural changes take place.
- The denominator of Eq. (12), $(\lambda_k - \lambda_l)$, shows that the contribution of eigenmode $\mathbf{x}_l$ to the sensitivity of eigenmode $\mathbf{x}_k$ reduces if the corresponding eigenvalue λ_l deviates more from eigenvalue λ_k.

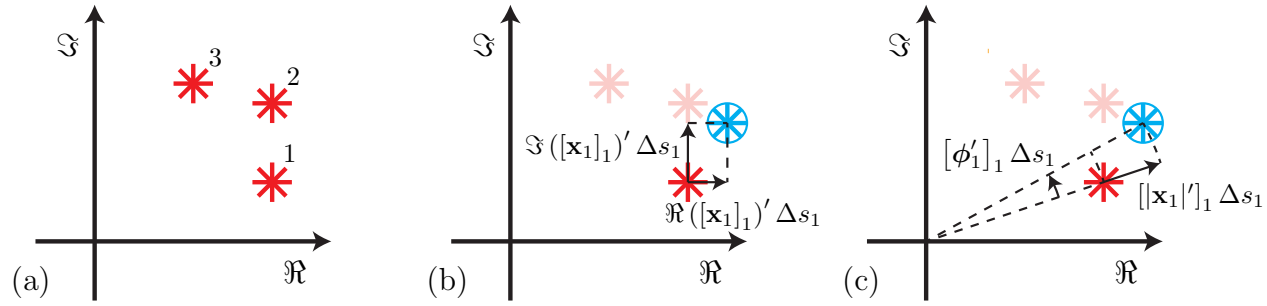

Figure 1: Illustrative sketch of the first eigenmode of a non-proportionally damped 3-dof system, visualized in the complex plane. (a) the non-synchronous nominal eigenmode, (b) change of dof 1 (i.e., towards encircled star) after a finite structural change, Δs_1, expressed in real and imaginary changes and, (c) change of dof 1 expressed in modulus and argument changes. The changes of dof 2 and 3 are not depicted for clarity reasons.

- The contribution of eigenmode $\mathbf{x}_k$ to the sensitivity of eigenmode $\mathbf{x}_k$ (see Eq. (13)) will be zero if the local structural modification introduces solely stiffness changes (i.e., $\mathbf{M}' = \mathbf{C}' = \mathbf{0}$ and $\mathbf{K}' \neq \mathbf{0}$). Eq. (13) arises from the applied normalization of the modes resulting in a scaling of the modes if either $\mathbf{M}'$ or $\mathbf{C}'$ is unequal to zero.

Since the eigenmode $\mathbf{x}_k$ is complex the eigenmode sensitivity, $\mathbf{x}_k'$, can be expressed by

$$\mathbf{x}_k' = \left[\Re\left(\mathbf{x}_k'\right) + i\Im\left(\mathbf{x}_k'\right)\right], \tag{16}$$

which shows modifications to the real and imaginary part. Figure 1a shows an illustrative sketch of the first eigenmode corresponding to a non-proportionally damped system, visualized in the complex plane. The change of dof 1 due to a finite control variable change Δs_1 can be approximated using Eq. (11) and Eq. (16) and is shown in Figure 1b. However, the interpretation is not straightforward since the eigenmode change leads to a relative shape and phase change of the dofs in the system.

2.4 Modulus and argument sensitivities

For a clear interpretation of the eigenmode sensitivity, the modulus and argument sensitivities of each dof are determined in this work. The modulus (see Eq. (7)) and argument (see Eq. (8)) sensitivity of a specific dof i to control variable s_1 is given by

$$[|\mathbf{x}_k|']_i = \frac{[\Re\left(\mathbf{x}_k\right)]_i\,[\Re\left(\mathbf{x}_k'\right)]_i + [\Im\left(\mathbf{x}_k\right)]_i\,[\Im\left(\mathbf{x}_k'\right)]_i}{\sqrt{\left([\Re\left(\mathbf{x}_k\right)]_i\right)^2 + \left([\Im\left(\mathbf{x}_k\right)]_i\right)^2}}, \tag{17}$$

leading to the modulus sensitivity set $|\mathbf{x}_k|' \in \mathbb{R}^N$, and

$$[\boldsymbol{\phi}_k']_i = \frac{[\Im\left(\mathbf{x}_k'\right)]_i\,[\Re\left(\mathbf{x}_k\right)]_i - [\Im\left(\mathbf{x}_k\right)]_i\,[\Re\left(\mathbf{x}_k'\right)]_i}{\left([\Re\left(\mathbf{x}_k\right)]_i\right)^2 + \left([\Im\left(\mathbf{x}_k\right)]_i\right)^2}, \tag{18}$$

leading to the argument sensitivity set $\boldsymbol{\phi_k}' \in \mathbb{R}^N$, respectively. With expression Eq. (16), the modulus and argument sensitivity can be determined after the eigenmode sensitivity is calculated. Figure 1c shows the approximated modulus and argument change of dof 1 due to a finite control variable change, Δs_1. The modulus sensitivity determines the change of the vibration shape and the argument sensitivity determine the change in leg/lead of a specific dof with respect to other dofs. This representation defines resonance mode changes in a much clearer way.

2.5 Resonance mode modification measure

In research on undamped resonance mode control, specific regions of the resonance mode have been selected at which the relative vibration amplitude needed to be maximized or minimized [13, 16]. To select these regions, a projection set was determined with non-zero entries at the locations which correspond to the spatial dofs at which the dynamic response needed to be modified. Control of non-proportionally damped resonance modes requires modifications to the relative magnitude and argument at specific regions.

To maximize or minimize the relative magnitude at a specific region, we define a similar normalized projection set (i.e., $\mathbf{b}^{\parallel} \in \mathbb{R}^N$). We obtain a quantitative measure of the nominal magnitude of the resonance mode, $|\mathbf{x}_k|$, at the locations of interest by projecting $|\mathbf{x}_k|$ onto the projection set $\mathbf{b}^{\parallel}$ resulting in a projection value $r_k^{\parallel}$ (i.e., $r_k^{\parallel} = \left(\mathbf{b}^{\parallel}\right)^T |\mathbf{x}_k|$). The modulus projection value sensitivity due to a structural change is given by

$$\left(r_k^{\parallel}\right)' = \left(\mathbf{b}^{\parallel}\right)^T |\mathbf{x}_k|'. \tag{19}$$

Whenever the relative magnitude at the location of interest needs to be maximized, the structural changes should be chosen such that Eq. (19) is maximized. Due to the normalization of the resonance modes (see Eq. (6)), the magnitude shape will change if the relative amplitude at a specific point is maximized or minimized.

Maximizing or minimizing the relative argument at a specific region within the structure is useless since the argument is not constrained or normalized like the magnitude. Hence, for argument control, we induce structural changes to modify the argument difference between dofs within the resonating structure. To minimize or maximize the argument difference between specific regions, we define a similar projection set (i.e., $\mathbf{b}^{\angle} \in \mathbb{R}^N$). Subsequently, we obtain a quantitative measure by projecting this projection set onto the nominal argument set of the resonance mode, $\boldsymbol{\phi}_k$, resulting in a projection value $r_k^{\angle}$ (i.e., $r_k^{\angle} = \left(\mathbf{b}^{\angle}\right)^T \boldsymbol{\phi}_k$). The argument projection value sensitivity due to a structural change is given by

$$\left(r_k^{\angle}\right)' = \left(\mathbf{b}^{\angle}\right)^T \boldsymbol{\phi}_k'. \tag{20}$$

Eq. (20) provides a tool to minimize/maximize the leg/lead of a specific dof (or region) with respect to another dof. The optimal local structural changes to modify resonance modes effectively in the desired way can be found by combining Eq. (19) and Eq. (20) into an optimization formulation.

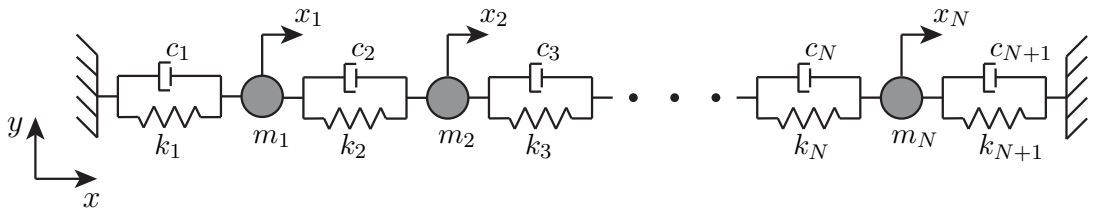

Figure 2: N-dof mass-spring-damper system with mass $m_i = 0.5$ kg for $i = 1, \ldots, N$, stiffness $k_j = 2$ N/m for $j = 1, \ldots, N+1$ and damping $c_n = 1$ Ns/m for $n = 1, \ldots, {}^{N}/_{2}$ and $c_n = 0$ Ns/m for $n = {}^{N}/_{2}+1, \ldots, N+1$. The longitudinal vibration (i.e., in x-direction) is represented by x_p for $p = 1, \ldots, N$.

3 NUMERICAL EXAMPLE

This section illustrates the presented systematic approach to modify non-proportionally damped resonating structures using a simple mass-spring-damper system. Firstly, the N-dof mass-spring-damper system is introduced together with some corresponding free vibration eigensolutions. After that, we present the projection sets to modify magnitude and argument at the locations of interest. With these projection sets, we identify the optimal locations to apply the local structural changes.

3.1 N-dof mass-spring-damper system

This example uses a simple clamped-clamped rod, represented by the N-dof mass-spring-damper system of Figure 2. The longitudinal vibrations (i.e., vibrations in x-direction) are investigated. However, the vibration modes will be presented in the y-direction for obvious visualization reasons. The number of dofs $N = 10$, the mass $m_i = 0.5$ kg for $i = 1, \ldots, N$, spring stiffness $k_j = 2$ N/m for $j = 1, \ldots, N+1$ and damping $c_n = 1$ Ns/m for $n = 1, \ldots, {}^{N}/_{2}$ and $c_n = 0$ Ns/m for $n = {}^{N}/_{2}+1, \ldots, N+1$. Hence, we have a non-proportionally damped mass-spring-damper system.

3.2 Free vibration eigensolutions

Since the system is non-proportionally damped, the eigenvalues and eigenmodes are complex. Table 1 compares the first 4 complex eigenvalues λ_k with their corresponding undamped eigenvalues ω_k. All complex eigenvalues have a negative real part indicating modal damping. The modal damping of the 2^{nd} eigenvalue is clearly larger. The damped eigenfrequency, represented by the imaginary part of the eigenvalues (i.e., $\Im(\lambda_k)$), deviates more from the undamped eigenfrequencies for higher eigensolutions.

Table 1: Comparison first 4 eigenvalues, undamped versus damped.

Eigenvalue	1	2	3	4
Undamped, ω_k	0.5693	1.1269	1.6617	2.1626
Damped, λ_k	$-0.0406 + 0.5693i$	$-3.6754 + 1.1135i$	$-0.1128 + 1.1746i$	$-0.4452 + 1.6423i$

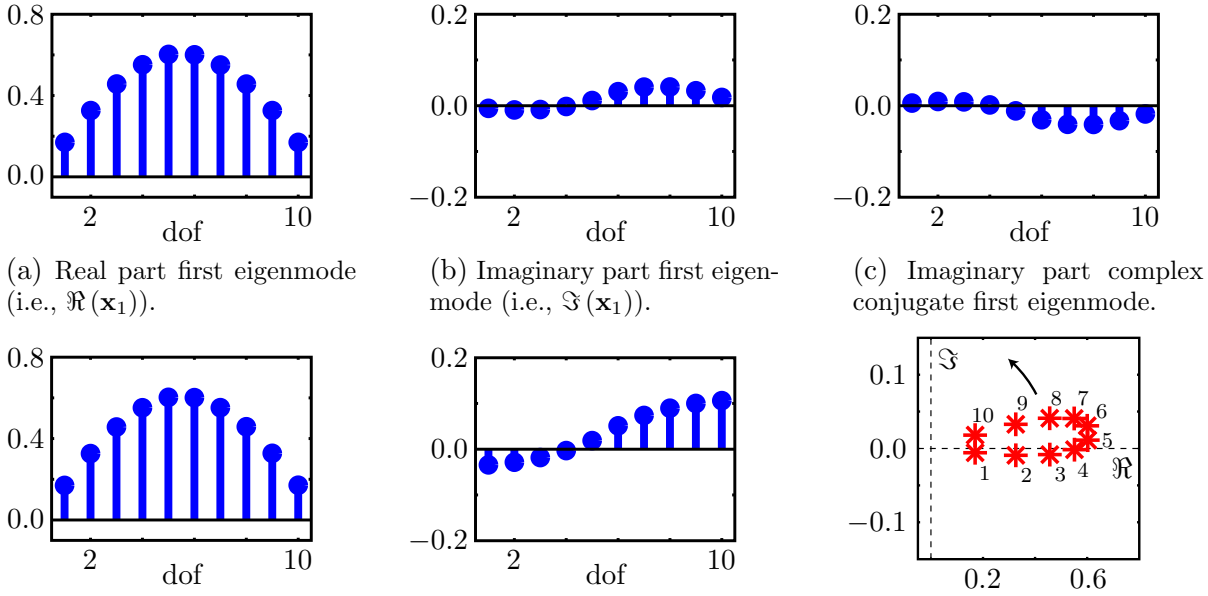

(a) Real part first eigenmode (i.e., $\Re(\mathbf{x}_1)$).

(b) Imaginary part first eigenmode (i.e., $\Im(\mathbf{x}_1)$).

(c) Imaginary part complex conjugate first eigenmode.

(d) Modulus (magnitude) first eigenmode (i.e., $|\mathbf{x}_1|$).

(e) Argument (phase) first eigenmode (i.e., $\boldsymbol{\phi}_1$).

(f) Rotation of the 10 dofs in a complex plane representation.

Figure 3: Different representations of eigenmode 1, $\mathbf{x}_1$.

Figure 3 shows different representations of the first eigenmode, $\mathbf{x}_1$. Figure 3a and Figure 3b show the real and imaginary part of the eigenmode, respectively. The imaginary part is clearly smaller compared to the real part. Figure 3c shows the imaginary part of the complex conjugate of eigenmode 1 (i.e., $\Im(\mathbf{x}_1^*)$) which shape is identical to the shape of Figure 3b apart from the minus sign. The real part of the complex conjugate of $\mathbf{x}_1^*$ is identical to the shape of Figure 3a. Figure 3d shows the modulus of the first eigenmode, $|\mathbf{x}_1|$, which looks comparable to the real part of the mode as shown in Figure 3a since the magnitude of the imaginary part is small. Figure 3e shows the corresponding argument, $\boldsymbol{\phi}_1$, showing the lag of the first dofs with respect to the other dofs during resonance. The Figures 3d and 3e determine the resonance mode behavior in a more insightful way. Figure 3f visualizes the different dofs of the resonance mode in the complex plane. During resonance, these dofs rotate around the origin, through the complex plane, while the argument difference between the dofs remains the same.

3.3 Projection set for magnitude and phase modifications

In this example, we aim to modify the modulus and argument of the first nominal resonance mode, $\mathbf{x}_1$, in a desired way. For the modulus, we specify dof 7 and 8 for which the relative modulus should be maximized. Figure 4a shows the defined normalized modulus projection set $\mathbf{b}^{\|}$. By projecting the modulus sensitivity onto this projection set (see Eq. (19)), we focus on the modulus sensitivity of these dofs only. For the argument, we

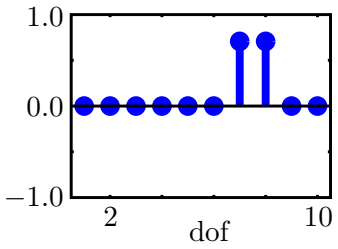

(a) Magnitude projection set (i.e., $\mathbf{b}^{\parallel}$)).

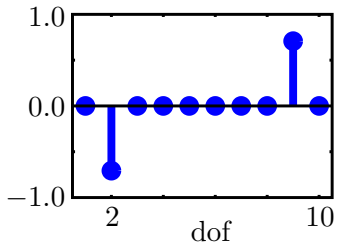

(b) Phase projection set (i.e., $\mathbf{b}^{\angle}$)).

Figure 4: Projection sets to select the region of interest for modulus and argument modifications.

want to maximize the argument difference between dof 2 and dof 9. Figure 4b shows the defined normalized argument projection set $\mathbf{b}^{\angle}$. By projecting the argument sensitivity onto this projection set (see Eq. (20)), we focus on the sensitivity of the argument difference between these dofs only.

3.4 Most effective location to modify structural property

For this example, we consider two different structural property changes to modify the resonance mode: (1) stiffness changes to modify the relative modulus, and (2) damping changes to modify the argument differences. For effective resonance mode control, we search for the locations at which the projection value sensitivity (see Eqs. (19) and (20)) is maximized due to the structural property changes. In this example we calculate sensitivities to the individual springs and dampers to find the most effective locations.

Figure 5a shows the spring dependent modulus projection value sensitivity, $(r_1^{\parallel})'$. The 11 sensitivity values are obtained by taking the sensitivity of the projection value to the individual springs k_j for $j = 1, \ldots, 11$. Figure 5a clearly indicates that the relative modulus of dof 7 and 8 is increased most effectively if positive stiffness changes are applied to the first few springs (i.e., spring 1, 2 and 3).

Figure 5b shows the damper dependent argument projection value sensitivity, $(r_1^{\angle})'$. The 11 sensitivity values are obtained by taking the sensitivity of the projection value to the individual dampers c_n for $n = 1, \ldots, 11$. Figure 5b clearly indicates that the argument difference between dof 2 and 9 is increased most if positive damping changes are applied to the first two dampers or if negative damping changes are applied to the last two dampers. However, negative damping changes of the last two dampers is not possible since the damping is already zero.

4 CONCLUSIONS

This work presents a systematic design approach to control non-proportionally damped resonance modes in an insightful way. This control is achieved using local structural property changes. The introduced modal basis gives enhanced insights in the possibilities and limitations of the potentially achievable changes of the resonance mode of interest.

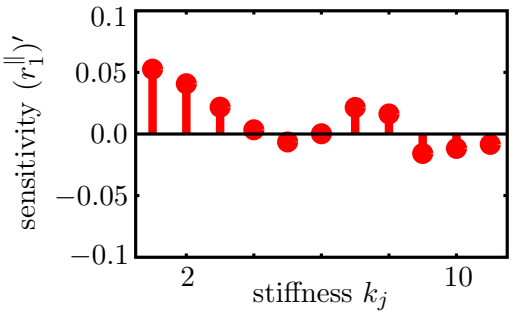

(a) Modulus projection value sensitivity (i.e., $(r_1^{\parallel})'$) to the individual stiffness values k_j for $j = 1, \ldots, 11$.

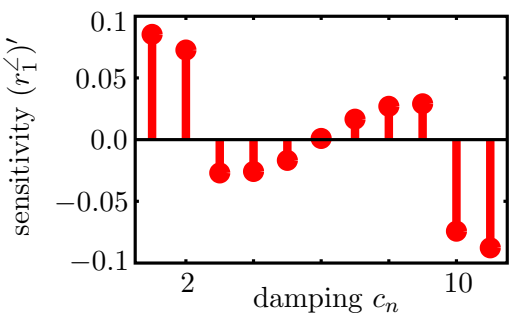

(b) Argument projection value sensitivity (i.e., $(r_1^{\angle})'$) to the individual damping values c_n for $n = 1, \ldots, 11$.

Figure 5: Structural property dependent projection value changes to determine the most effective spot to induce local structural property changes to modify the resonance mode in the desired way.

If the number of dofs of the system increases, the eigenmode sensitivity (and, hence, the modulus and argument sensitivity) appears to be mainly determined by neighboring eigensolutions. Hence, a limited number of eigensolutions is required during the analysis which reduces the computational effort.

Eigenmodes of non-proportionally damped systems are complex which complicates the interpretation. This is caused by the fact that both the real and imaginary part of the eigenmode contain information. The modulus (magnitude) and argument (phase) of each eigenmode appear to be much more insightful in interpreting complex eigenmodes and eigenmode modifications due to local structural changes.

Projection sets are defined to specify the regions at which the resonance mode should be modified. These projection sets allow to specify: (1) the locations at which the relative modulus of a specific resonance mode should be changed, and (2) the regions for which the argument difference should be modified. Hence, non-proportionally damped resonance modes can be modified in a systematic and intuitive manner.

Future work will focus on the response modifications of non-proportionally damped systems which are harmonically driven at a frequency which is very close to one of the structural eigenfrequencies.

REFERENCES

[1] Calmes S., Schweizer, P. and Renaud P. Resonating large angle and low consumption micromachined optical scanner. In: *Proceedings of SPIE - The International Society for Optical Engineering* (1998) Motamedi M.E., Goring R. (ed.) **3276**: 96 – 102, doi:10.1117/12.302413, Jan. 1998 - San Jose, CA.

[2] Greenewalt, C.H. The Wings of Insects and Birds as Mechanical Oscillators, *Proceedings of the American Philosophical Society* (1960) **104**(6):605–611.

[3] Wood, R.J. The First Takeoff of a Biologically Inspired At-Scale Robotic Insect. *IEEE Transactions on Robotics* (2008) **24**(2):341–347, doi:10.1109/TRO.2008.916997.

[4] Bolsman, C.T., Goosen, J.F.L. and van Keulen, F. Design Overview of a Resonant Wing Actuation Mechanism for Application in Flapping Wing MAVs. *International Journal of Micro Air Vehicles* (2009) **1**(4): 263–272, doi:10.1260/175682909790291500.

[5] Crawley, E.F. and de Luis, J. Use of Piezoelectric Actuators as Elements of Intelligent Structures. *AIAA Journal* (1987) **25**(10):1373–1385, doi:10.2514/3.9792.

[6] Fox, R.L. and Kapoor, M.P. Rates of Change of Eigenvalues and Eigenvectors. *AIAA Journal* (1968) **6**(12):2426–2429, doi:10.2514/3.5008.

[7] Nelson, R.B. Simplified Calculation of Eigenvector Derivatives. *AIAA Journal* (1976) **14**(9):1201-1205.

[8] Adhikari, S. Rates of change of eigenvalues and eigenvectors in damped dynamic system. *AIAA Journal* (1999) **37**(11):1452–1458, doi:10.2514/2.622.

[9] Adhikari, S. and Friswell, M.I. Eigenderivative analysis of asymmetric non-conservative systems. *International Journal for Numerical Methods in Engineering* (2001) **51**(6):709–733, doi:10.1002/nme.186.

[10] Friswell, M.I. and Adhikari, S. Derivatives of complex eigenvectors using Nelson's method. *AIAA Journal* (2000) **38**(12):2355–2357, doi:10.2514/2.907.

[11] Adhikari, S. Derivative of Eigensolutions of Nonviscously Damped Linear Systems. *AIAA Journal* (2002) **40**(10):2061–2069, doi:10.2514/2.1539.

[12] Adhikari, S. and Friswell, M.I. Calculation of Eigensolution Derivatives for Non-viscously Damped Systems Using Nelson's Method. *AIAA Journal* **44**(8):1799–1806, doi:10.2514/1.20049.

[13] Maeda, Y. and Nishiwaki, S. and Izui, K. and Yoshimura, M. and Matsui, K. and Terada, K. Structural topology optimization of vibrating structures with specified eigenfrequencies and eigenmode shapes. *International Journal for Numerical Methods in Engineering* (2006) **67**(5):597–628, doi:10.1002/nme.1626.

[14] Rubio, W.M. and Paulino, G.H. and Silva, E.C.N. Tailoring vibration mode shapes using topology optimization and functionally graded material concepts. *Smart Materials and Structures* (2011) **20**(2) art. no. 025009, doi:10.1088/0964-1726/20/2/025009.

[15] Tsai, T.D. and Cheng, C.C. Structural design for desired eigenfrequencies and mode shapes using topology optimization. *Structural and Multidisciplinary Optimization* (2013) **47**(5):673–686, doi:10.1007/s00158-012-0840-2.

[16] Peters, H.J. and Goosen, J.F.L. and Tiso, P. and van Keulen, F. Control of Harmonically Driven Resonating Compliant Structures using Local Structural Modifications. In: *ECCO-MAS Multibody Dynamics* (2013) Terze Z., Vrdoljak M. (ed.), ISBN: 978-953-7738-22-8, July - Zagreb, Croatia.